Process integration for efficient conversion of cassava peel waste into polyhydroxyalkanoates

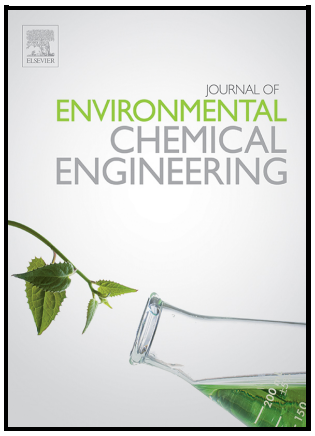

Carmen Hierro-Iglesias, Cornelius O. Fatokun, Annie Chimphango, Richard Bayitse, Paula Helena Blanco-Sanchez, Patricia Thornley, Alfred Fernandez-Castane

PII: S2213-3437(23)02554-X

DOI: https://doi.org/10.1016/j.jece.2023.111815

Reference: JECE111815

To appear in: *Journal of Environmental Chemical Engineering*

Received date: 26 July 2023
Revised date: 20 December 2023
Accepted date: 23 December 2023

Please cite this article as: Carmen Hierro-Iglesias, Cornelius O. Fatokun, Annie Chimphango, Richard Bayitse, Paula Helena Blanco-Sanchez, Patricia Thornley and Alfred Fernandez-Castane, Process integration for efficient conversion of cassava peel waste into polyhydroxyalkanoates, *Journal of Environmental Chemical Engineering,* (2023) doi:https://doi.org/10.1016/j.jece.2023.111815

Process integration for efficient conversion of cassava peel waste into polyhydroxyalkanoates

Carmen Hierro-Iglesias [a], Cornelius O. Fatokun [a,b], Annie Chimphango [c], Richard Bayitse[d], Paula Helena Blanco-Sanchez [a], Patricia Thornley [a] and Alfred Fernandez-Castane *[,a]

[a]Energy and Bioproducts Research Institute, Aston University, Birmingham, B4 7ET, UK

[b] Department of Biochemistry, School of Life Sciences, Federal University of Technology, Akure 340252, Ondo State, Nigeria

[c]Department of Process Engineering, University of Stellenbosch, Private Bag X1, Stellenbosch 7602, South Africa

[d] Council for Scientific and Industrial Research/Institute of Industrial Research, P.O Box LG 576, Legon, Ghana

*Correspondence to: Energy and Bioproducts Research Institute & Aston Institute of Materials, Research, Aston University, Birmingham, B4 7ET, UK, a.fernandez-castane1@aston.ac.uk

Abstract

Polyhydroxyalkanoates (PHA) are biodegradable polyesters that can be produced from renewable resources. However, PHA biomanufacturing is costly compared to petrochemical-based plastics. A promising solution consists of using cassava (*Manhiot esculenta*) waste, abundant biomass in developing countries, as a carbon source for PHA production. This study involved characterising untreated and acid-hydrolysed cassava peel (CP) to confirm the degradation of polysaccharides into fermentable sugars after pre-treatment. A

chemical and biological integrated process was developed, optimising the pre-treatment using a central composite design. The highest conversion of CP into reducing sugars was 97% (w/w) using 3 M H_2SO_4, 120 min and 90 ºC. The ability of *Cupriavidus necator* to grow on CP hydrolysate and produce PHA was screened resulting in up to OD_{600} 15.8 and 1.5 g/L of PHA (31% (g_{PHA}/g_{DCW})). Flow cytometry allowed rapid, simple, and high-throughput assessment of PHA content. These findings pave the way for developing a biorefinery platform for PHA production from cassava waste.

Graphical abstract

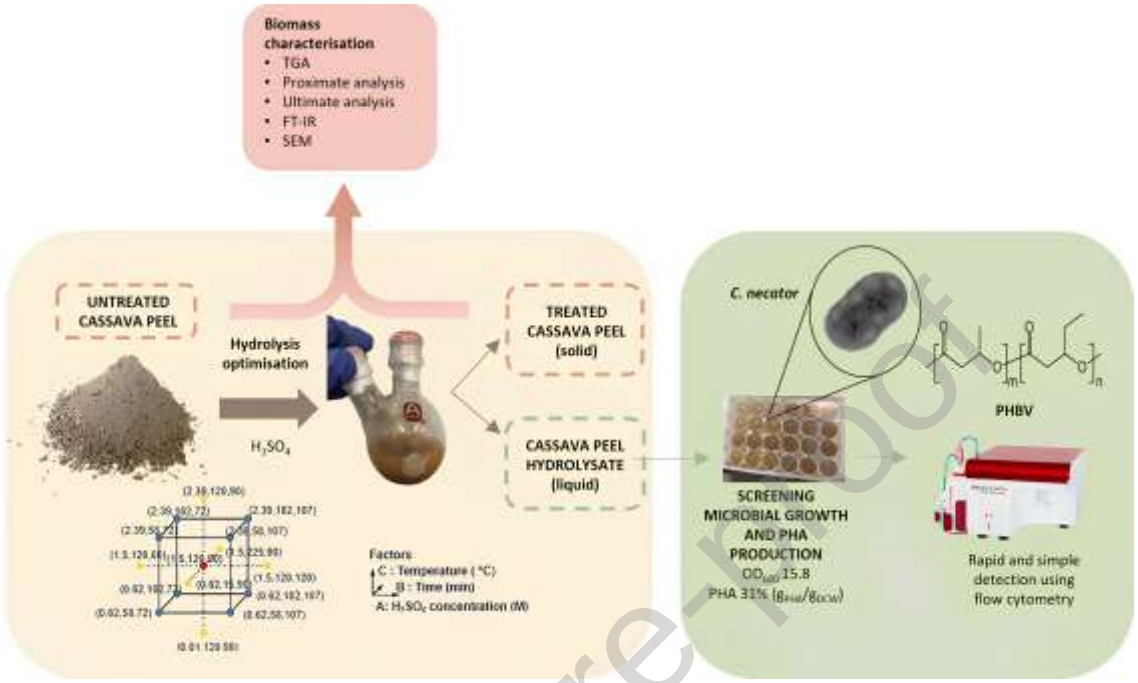

Keywords

Polyhydroxyalkanoates, cassava, acid hydrolysis, waste valorization,

Cupriavidus necator

1. Introduction

Biomass can be used as a renewable energy and bioproduct source, but its competition with food represents a challenge [1]. About 13% of the global cropland is currently used to produce first-generation biofuels and textiles, having significant ethical and economic concerns [2], and negatively affecting vulnerable populations [3]. Second-generation biomass which comprises biomass waste instead of edible crops is a promising alternative to alleviate social impacts and environmental pollution [4].

Cassava (*Manhiot esculenta*) is a crop primarily grown in tropical and subtropical regions. Significant cassava waste is produced in its processing, whereby cassava peel (CP) constitutes around 20% of the total waste [5,6]. CP is valuable

due to its high starch, cellulose, and hemicellulose content. These components can be hydrolysed into fermentable sugars (e.g., glucose, xylose, etc) which can be used to co-produce bioenergy and various bio-based products such as biopolymers [7]. However, to effectively use waste biomass for bioenergy and bioproducts production, it is important to understand its characteristic properties, which can vary depending on factors such as the variety, source, and treatment method [8]. Characterizing biomass involves evaluating its chemical, physical, and thermal properties such as proximate and ultimate analysis, elemental composition, particle size distribution, bulk density, and moisture content [9,10]. Multiple and orthogonal characterization methods are necessary to obtain a comprehensive understanding of biomass and accurately evaluate its potential. Furthermore, utilizing biomass waste in its natural form for bio-based products production is challenging due to its hygroscopic nature, high bulk volume, and low heating value, resulting in inefficient and costly processes [11]. Therefore, biomass pre-treatment is essential to enable conversion into value-added products [12]. For example, acid hydrolysis is commonly used to convert biomass into fermentable sugars. Conversions of 66% [13] and 95% [14] were achieved from CP to reducing sugars using H_2SO_4 0.1 M and 1.5 M, respectively. HCl 0.25 M was tested on cassava bagasse reaching 63% conversion [13]. However, systematic approaches to converting cassava waste into fermentable sugars are scarce.

Fermentable sugars obtained from biomass can be upgraded into polyhydroxyalkanoates (PHA). These biopolymers are a promising alternative to petroleum-based plastics [15], as they can be synthesized from renewable resources and biodegraded by microorganisms [16]. PHA are produced by

microbes and stored as cytoplasmic granules [17], providing carbon and energy to the cell during starvation [18,19]. Additionally, PHA enhances stress resistance and robustness of microbes when exposed to diverse environmental stressors, including but not limited to high or low temperature, freezing conditions, oxidative stress, and osmotic pressure [20]. There are over 100 different PHA monomers [21], and poly(3-hydroxybutyrate) (PHB) is the most common [17]. PHA can be used in a broad range of applications such as packaging, agricultural use, and medical applications [22–25]. *Cupriavidus necator (C. necator)* is the model organism for PHA production under nutrient stress, such as nitrogen or phosphorous limitation. This microorganism natively produces PHA, eliminating the requirement for genetic engineering [26].

However, PHA commercialization is hindered by the high manufacturing cost [24], which is 3 to 4-fold higher compared to petrochemical-derived plastics [38]. The cost of carbon sources represents 40% of the total operating cost, and waste biomass provides an opportunity to reduce expenses [27]. Studies have shown PHA concentrations up to 52% (g_{PHA}/g_{DCW}) using waste biomass such as sugar cane molasses and corn cob [28,29]. Few studies have used cassava waste to produce PHB [7]. However, to the best of our knowledge, no other type of PHA has been produced using cassava waste to date. Furthermore, such studies are very scarce and typically involve the supplementation of additional nutrients, and the utilization of genetically modified strains, thereby increasing the overall process cost. Consequently, the potential of cassava waste as the sole carbon source for PHA production using *C. necator* represents a gap in research.

This study aims to develop an integrated chemical and biological process for PHA production from CP waste. Here, we provide an in-depth characterization of

untreated and acid-hydrolysed CP, and an optimization of the acid hydrolysis into fermentable sugars using diluted H_2SO_4. For the hydrolysis optimization, the interaction between acid concentration, hydrolysis time, and hydrolysis temperature, was investigated systematically using a design of experiments (DoE). Additionally, *C. necator* was screened for growth and PHA production using cassava peel hydrolysate (CPH).

2. Materials and methods

2.1 Feedstock and feedstock pre-treatment

Cassava peel (CP) was collected from a small cassava processing plant in Bawjiase, Ghana. CP was subsequently dried overnight at 60 ºC before being milled. Subsequently, the total carbohydrate composition was determined, being 88%, as described elsewhere [30]. All chemicals and materials used in this study were purchased from Fisher Scientific (Loughborough, UK) unless specified.

CP was pre-treated using acid hydrolysis to release fermentable sugars. For characterization purposes, CP was hydrolysed with 0.6 M H_2SO_4 (>95%, CAS 7664-93-9), at 107 °C for 58 min. These conditions enable high conversion (82%) from CP to total reducing sugars (TRS) while preserving a non-converted portion (18%) for characterization purposes. The optimization study used a combination of the H_2SO_4 concentrations, hydrolysis times, and temperatures as presented in Table 1. The reactions were performed using 20 mL of a solution containing 10% (w/v) of cassava peel in two-neck round bottom 50 mL pressure flasks (Aldrich®, Merck, Darmstadt, Germany). The hydrolysis reactions were carried out d in a Starfish workstation (Radleys, Essex, UK). Experiments carried out below 100 ºC were fitted with a condenser to avoid

sample loss due to evaporation. To achieve temperatures above 100 ºC, the flasks were sealed to maintain them pressurised. Subsequently, the samples were vacuum filtered through an 11 µm cellulose filter paper (Whatman, Cytiva, Washington D.C, United States), resulting in solid (treated CP) and liquid fractions (CPH). The solid fraction was air-dried and stored at room temperature until analysis. The liquid fraction, constituting the CPH was neutralized to pH 7 using 12.5 M NaOH. 1 mL aliquots were stored at -20 °C for sugars analysis. CPH for culture media were sterilized by vacuum filtration through a 0.2 µm polyethersulfone (PES) filter and stored at room temperature.

2.2 Cassava peel characterization

2.2.1 Thermogravimetric analysis

A thermogravimetric analyser TGA/DSC3+ STARe System (METTLER TELEDO, Ohio, USA) was utilized to assess the thermal properties of both untreated and treated CP. Alumina crucibles were loaded with 3 mg of each sample and subjected to a temperature range from 25 to 900 °C at a heating rate of 10 °C/min under a nitrogen atmosphere (30 mL/min) to maintain an inert atmosphere. The sample mass was recorded and used to determine the mass loss and mass loss rate percentage as follows:

$$\text{Mass loss } (\%\ \text{w/w}) = \frac{\text{Mass of sample}}{\text{Mass sample 25°C}} \text{ x } 100 \quad \text{(Eq.1)}$$

$$\text{Mass loss rate } (\%\ \text{w}/(\text{w min})) = \frac{\Delta\text{mass}}{\Delta\text{time}} \text{ x } 100 \quad \text{(Eq.2)}$$

2.2.2 Proximate and ultimate analysis

Data obtained from the TGA was used for the proximate analysis to determine moisture and volatile matter as follows [31]:

$$\text{Moisture (\%w/w)} = \frac{\text{Mass of sample at 25 °C- Mass of sample at 105 °C}}{\text{Mass of sample at 25 °C}} \times 100 \quad \text{(Eq. 3)}$$

$$\text{Volatile matter (\%w/w)} = \frac{\text{Mass of sample at 105 °C- Mass of sample at 900 °C}}{\text{Mass of sample at 105 °C}} \times 100 \quad \text{(Eq.4)}$$

Ash content was determined by the ignition of samples in a muffle furnace at 575 °C for 3 h according to ASTM E-1755-01 standard method. The remaining residue after combustion of the organic material represented the ash content and was calculated as follows [31]:

$$\text{Ash content (\%w/w)} = \frac{\text{Mass of sample at 575 °C}}{\text{Mass of sample at 105 °C}} \times 100 \text{ (Eq. 5)}$$

The fixed carbon (FC) was calculated as follows [31]:

FC (%w/w))= 100 - (moisture (%)+ volatile matter (%)+ ash (%)) (Eq. 6)

Ultimate analysis was carried out to determine the elemental composition. A FLASH 2000 CHNS/O analyser (ThermoFisher, Waltham, USA) was used to determine Carbon (C), Hydrogen (H), Nitrogen (N), and Sulphur (S) content. The oxygen (O) content in the cassava peel samples was determined by difference (Eq. 7).

O (%w/w))= 100 - (C (%)+ H (%)+ N (%) + S (%)) (Eq. 7)

2.2.3 Functional group analysis

Fourier transform infrared (FT-IR) spectroscopy was carried out using a NICOLET iS50 (ThermoFisher, Waltham, USA) equipped with attenuated total reflectance (ATR) to characterise chemical functional groups. Spectra were recorded at a wavenumber range of 400 – 4000 cm^{-1} at a resolution of 4 cm^{-1}.

2.2.4 Surface morphology analysis

The surface morphology of the untreated and treated CP was evaluated using scanning electron microscopy (SEM, JSM-7800F Prime, JEOL, Japan). Images were acquired at 1200x magnification at 5.0 kv.

2.3 Experimental design

Optimisation of CP hydrolysis was carried out to maximise the release of fermentable sugars. Solids concentration was selected based on previous cassava acid hydrolysis studies [32–34].

A design of experiments (DoE) based on a central composite design (CCD) and response surface methodology (RSM) was used to determine optimum CP hydrolysis conditions. The effect of three variables (H_2SO_4 concentration (*[H_2SO_4]*, M); time (*t*, min); and temperature (*T*, ºC)) was evaluated on the response (*TRS* concentration (g/L).

Table 1 shows the independent variables and levels used in the design. Central points were repeated six times to obtain a close approximation of the experimental error. The independent variables and their ranges were guided by preliminary experiments (not published) and literature data [13,14].

Table 1. Independent variables and their levels used in the central composite design (CCD).

Independent variables	Units	Notation	Factor level				
			-1.68	-1	0	1	1.68
H_2SO_4 concentration ([H_2SO_4])	M	x_1	0.01	0.60	1.50	2.40	3.00
Time (t)	Min	x_2	15	58	120	182	225
Temperature (T)	ºC	x_3	60	72	90	108	120

Experiments were conducted towards the construction of a mathematical model. The TRS concentration (*y*) was determined using the following polynomial equation [35]:

$$y=\beta_0+\sum_{i=1}^{k}\beta_i X_i+\sum_{i=1}^{k}\beta_{ii}X_i^2+\sum_{i=1}^{k}\sum_{i,j}^{k}\beta_{ij}X_iX_j \qquad \text{(Eq. 8)}$$

where y is the response variable; x_i, x_j, and x_k are the corresponding actual values of the variables; β_0 is the regression coefficient of the fitted response at the centre point of the design; β_i is the linear term coefficient, β_{ii} is the regression coefficient for quadratic effects and β_{ij} and β_{ji} are the interaction terms coefficients.

Subsequently, non-significant terms were removed from the equation using the backward elimination methodology, followed by the addition of higher degree factors to the polynomial equation [36]. The effect and regression coefficients of individual linear, quadratic, and interaction terms were determined using analysis of variance (ANOVA). The RSM was applied to the experimental data using the commercial statistical package Design-Expert version 11.1.2.0. A confidence interval of 95% was chosen, hence p-values lower than 0.05 were considered statistically significant [37].

2.4 Total reducing sugars (TRS) determination

TRS concentration in CPH was carried out using the DNS (Di-nitrosalicylic acid) test, adapted from Miller (1959) [38]. The DNS reagent composition was as follows (% (w/v)): 0.63 DNS; 0.5 NaOH; 18.2 $KNaC_4H_4O_6 \cdot 4\ H_2O$; 0.5 $Na_2S_2O_5$ and 0.5 % (v/v) C_6H_6O. 0.5 mL of sample was mixed with 0.5 mL of DNS reagent and subsequently, boiled in water for 5 min and cooled down to room temperature. Absorbance was measured at 575 nm using a Jenway 6310 Spectrophotometer (Keison Products, Chelmsford, UK). Absorbance values were interpolated to calculate sample concentrations based on a calibration curve prepared using pure synthetic D-(+)-glucose (CAS 2280-44-6).

2.5 Strain and microbial cultivation

Cupravidus necator (C. necator) H16 was used to perform the biotransformation from sugars to PHA. *C. necator* H16 was originally a fructose consumer. However, for the purposes of our research, it was mutated to obtain a glucose-utilizing strain via adaptive evolution. Bacteria and mutation protocol were kindly provided by Dr. Katalin Kovacs of the University of Nottingham (October 2019). Screening of microbial growth using CPH as a sole source of nutrients was carried out in triplicates using 24-well microplates using 1 mL of neutralized CPH inoculated at OD_{600} 0.1 and incubated for 48 h, 30 ºC and 250 rpm in a shaker incubator (Incu-Shake MAXI®, SciQuip Ltd, Newtown, UK). For the inoculum, one loop of cryostock, stored at - 80 ºC in 15% (w/w) glycerol, was aseptically transferred into 10 mL of inoculum media containing (g/L): 10, peptone; 10, beef extract and 5, NaCl. The pH of the medium was adjusted to 7 using NaOH 1 M and subsequently sterilised by autoclaving at 121 ºC for 20 min. Inoculums were cultured overnight at 30 ºC and 250 rpm in a shaker incubator (Incu-Shake MAXI®, SciQuip Ltd, Newtown, UK).

2.6 Screening of microbial growth and PHA production

Microbial growth was analysed by optical density at a wavelength of 600 nm using a Jenway 6310 Spectrophotometer (Keison Products, Chelmsford, UK). PHA determination from microtiter samples was adapted from elsewhere [18]. Briefly, bacterial samples were resuspended in phosphate-buffered saline (PBS) and stained with pyrromethene-546 (Pyr-546) (Exciton, Lockbourne, USA). Pyr-546 stocks were stored at -20 ºC in DMSO and added to the bacterial solution at a concentration of 5 µg/mL. Stained samples were incubated for 1 min and

analysed with a flow cytometer BD Accuri™ C6 Plus Flow Cytometer (Becton, Dickinson and Company, Oxford, UK) using a 488 nm solid-state laser. Fluorescence was detected using a 533/30 BP filter (FL1-A) .

A correlation between PHA concentration (%) quantified using GC-MS and fluorescence values from Pyr-546-stain cells, was performed to calculate the concentration of PHA from FCM data and are available in the Supplementary materials.

PHA quantification was performed by acid propanolysis followed by GC-MS analysis, adapted from elsewhere [39].

The bacterial pellet was freeze-dried in a Lablyo benchtop freeze dryer (Frozen in Time Ltd, York, UK) at -50 °C and 1-5 Pa, overnight. Propanolysis was performed using 5 mg of lyophilized bacteria in 1 mL of chloroform and 1 mL of 1-propanol containing 15% of 37% (v/v) HCl in an 8 mL glass tube (Duran®, Mainz, Germany). 50 µL of 1 mg/mL solution of benzoic acid in 1-propanol was added as the internal standard. The mixtures were incubated for 2 h at 100°C in an oven (Memmert, Schwabach, Germany). After cooling to room temperature, 1 mL of distilled water was added followed by vortexing for 30 s, and left standing for 5 min to allow for phase separation. The upper aqueous phase was discarded, and the washing step was repeated to eliminate impurities. 1 mL of the organic phase containing derivatised PHA was filtered with 0.2 µm nylon filters and transferred to a GC-MS vial. The standard sample of poly(3-hydroxybutyric acid-*co*-3-hydroxyvaleric acid) (PHBV, PHV content 8 mol % 80181-31-3, Merck, Darmstadt, Germany) was used to prepare the standard calibration curve. Analysis was performed using a Single quadrupole gas chromatograph-mass spectrometer GCMS-QP2010 (Shimazu, Milton Keynes,

UK). One µL was injected into an analyser with a 30 m SH-Rtx-5MS column (Shimazu, Milton Keynes, UK) at 280°C. The flow rate was set at 1.25 mL/min and the ionization detector at 240°C. Column temperature was programmed from 40 to 250°C at a rate of 5°C/min. The total measurement time for each sample was 40 min. PHBV was identified using the internal libraries NIST17s and NIST17-1 available in GC-MS Postrun Analysis Software (Shimazu, Milton Keynes, UK). PHBV amount of each sample was normalised by the weight of the lyophilised bacteria and expressed as a percentage of polymer weight/cell dry weight.

3. Results and discussion

3.1 Cassava peel characterization

3.1.1 Thermal characterization

Thermogravimetric (TGA) and differential thermogravimetric (DTG) curves for untreated and treated CP are presented in Figure 1.

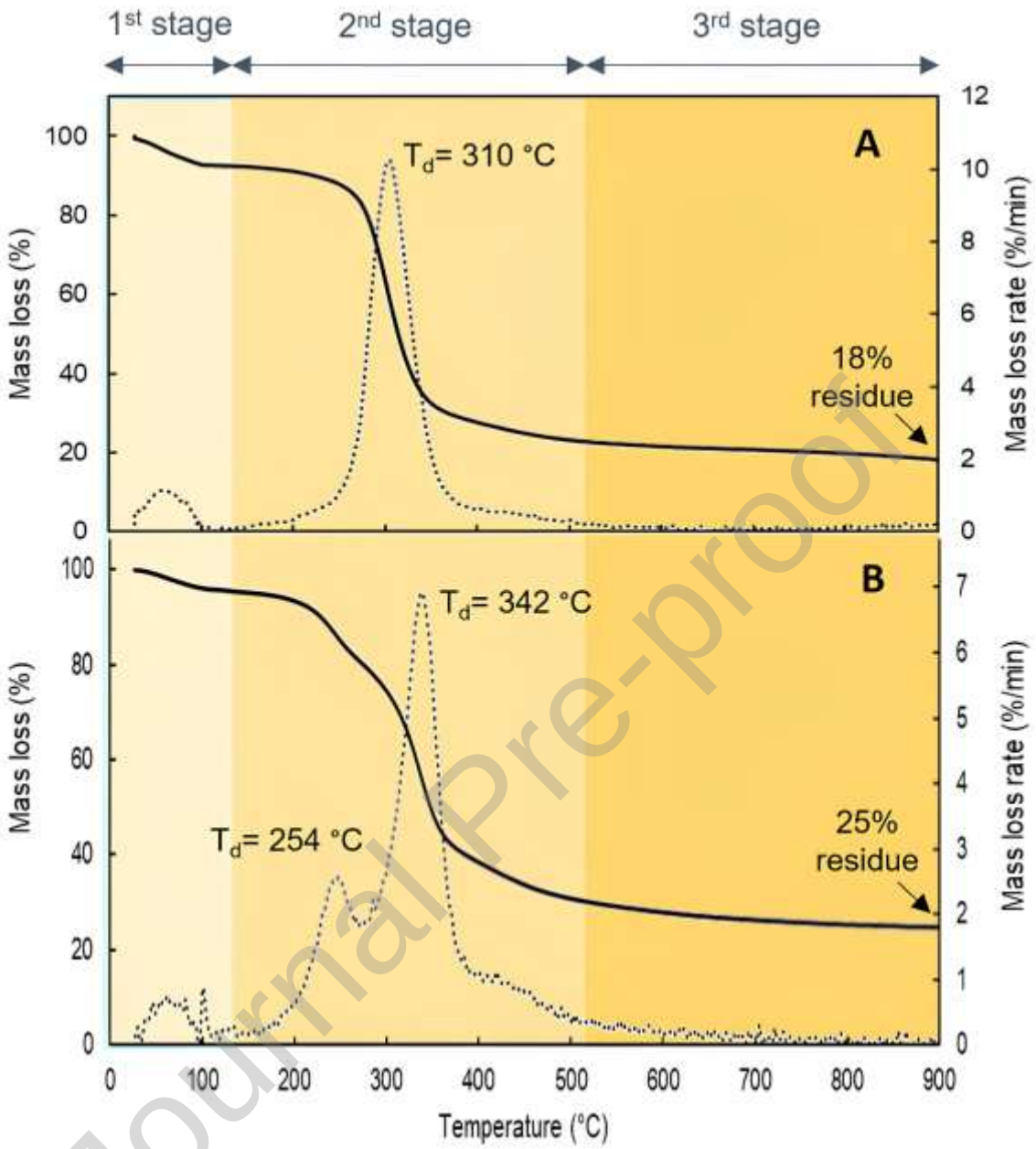

Figure 1. Thermogravimetric (black line) and derivative thermogravimetric (dotted line) curves of untreated (A) and treated (B) cassava peels. T_d: degradation temperature.

Results reveal three primary stages of degradation, stage 1 (25-150 °C), stage 2 (150-450 °C), and stage 3 (450-900 °C). Stage 1 (25 – 150 °C) shows a 4% mass loss in both samples, which can be attributed to the evaporation of

humidity and degradation of light compounds [40]. The sharper peak emerging in the treated CP at 100 °C may correspond to the degradation of light compounds, such as sulfur groups, that appeared after the acid hydrolysis.

Stage 2 (150 to 450 °C) corresponds to the degradation of volatile substances, such as hydrocarbons, H_2, CO, CH_4, and incombustible gases [41], including the major constituents of cassava (starch, cellulose, hemicellulose, and lignin), showing a degradation temperature (T_d) of 310 °C. Both samples exhibited a weight loss of approximately 60% in stage 2 (Figure 1) [60]. In Figure 1A, the presence of a single peak (150 to 450 °C) is likely due to overlapping degradation temperatures of cassava constituents [42].

In contrast, the treated CP displayed two degradation temperatures (T_d), in Stage 2, at 254 and 342 °C (Figure 1B). This can be explained by the presence of less thermally stable components resulting from the acid hydrolysis whereby CP composition undergoes changes due to the breakdown of complex carbohydrates into simpler sugars. For example, the appearance of a peak at 254 °C might correspond to the degradation of simpler sugars formed during acid hydrolysis, whereas the peak at 352 °C might be related to the degradation of remaining components, such as starch, cellulose, or lignin, in the treated CP [43]. Furthermore, the potential incomplete degradation of biomass cross-linkages between lignin and cellulose and hemicellulose can affect the degradation temperature, causing a shift in the curves towards higher temperatures compared to the untreated sample [44].

Stage 3 (450 to 900 °C) is often associated with char formation. A biomass loss of 12% and 13% was observed for untreated (Figure 1A) and treated (Figure 1B) CP, respectively. The loss of mass corresponds to the degradation of the

remaining lignin, and minerals, and the production of char following devolatilisation [45].

A remaining residue of 18% and 25% was observed for untreated and treated CP, respectively (Figure 1). The increased residue in the treated CP may be due to the effect of the acid hydrolysis on the CP constituents. Lignin has higher thermal stability than starch, cellulose, and hemicellulose. Therefore, when the treated biomass is subjected to TGA, the remaining lignin contributes to a higher overall residue than the untreated biomass and these observations are in agreement with previous studies [46].

Overall, the primary organic materials in cassava peels were decomposed below 450 °C and these findings are consistent with previous studies suggesting temperatures around 500 °C for thermal degradation of cassava [42,45].

3.1.2 Proximate and ultimate analysis

Figure 2A presents the proximate analysis of CP, including moisture content, volatile matter, ash content, and fixed carbon composition. The treated CP had a lower moisture content (3.8%) than the untreated CP (7.4%). Idris et al. reported similar moisture content as the treated CP [47]. Other works also reported comparable moisture contents for the untreated CP [45,48–50]. The moisture content of biomass can be variable, as it depends on different conditions such as storage, drying conditions, and variety of feedstock.

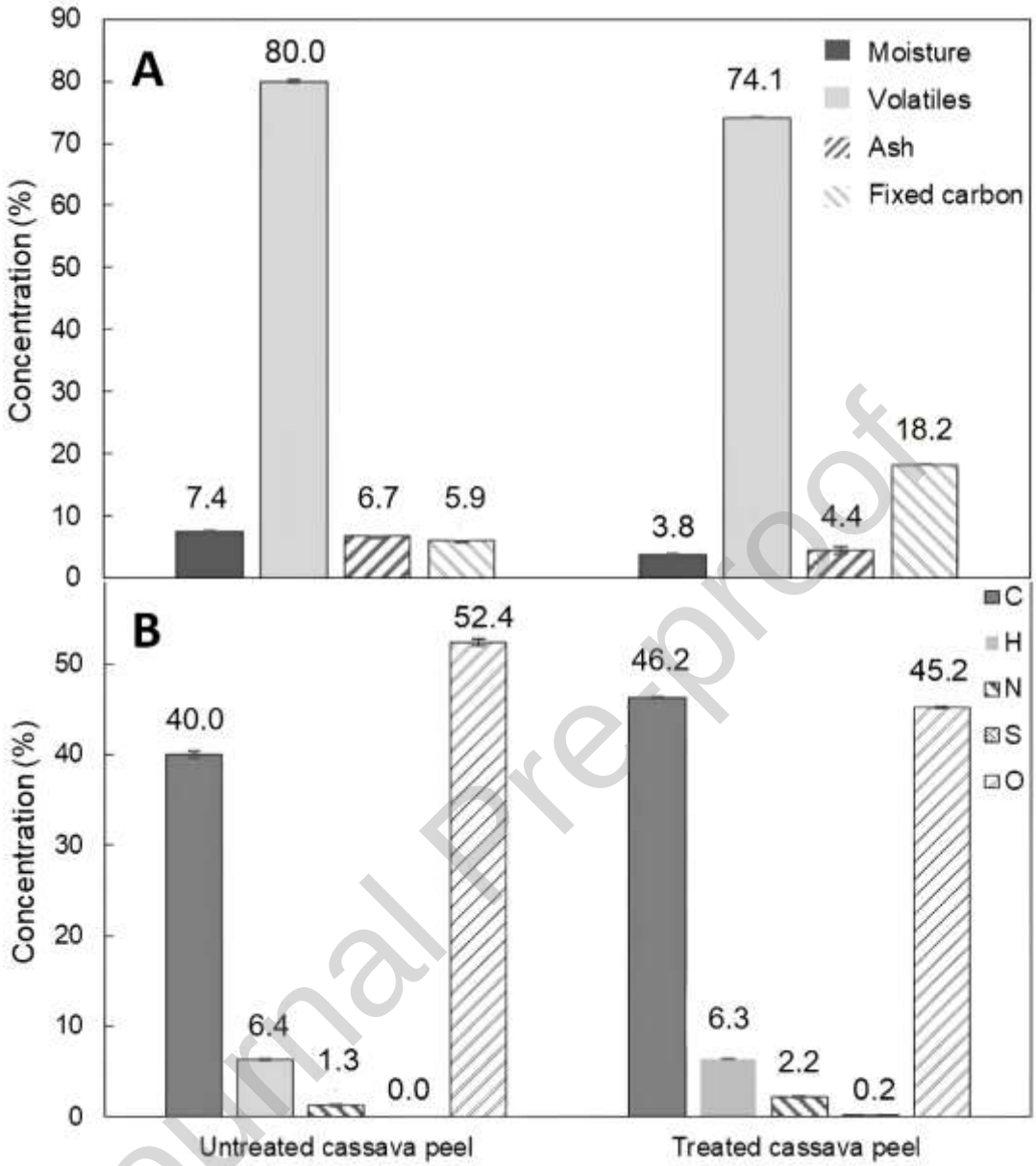

Figure 2. Proximate (A) and ultimate (B) properties of untreated and treated cassava peels (n=3).

The moisture content from the proximate analysis was compared to the TGA analysis (Figure 1) results, showing 4% moisture content in both samples. The treated CP exhibited consistent moisture content between TGA and proximate analysis. However, the untreated CP had a moisture content of 7.4% in proximate analysis.

The untreated and treated CP showed volatile matter concentrations of 80 and 74%, respectively. TGA analysis estimated a volatile content of approximately 60% for both samples (Figure 1). The variation is attributed to differences in the methodology used in each technique. The volatile matter results in Figure 2A align with most values documented in the literature [42,48,51]. Due to the influence of various factors, such as the origin and processing, on volatile matter content, it is critical to characterize biomass for optimal utilization [52]. The ash concentration of untreated and treated CP was 6.7% and 4.4%, respectively, consistent with previous studies [48,53–56]. Other studies found an 8-19% decrease in ash content when the peels were subjected to hydrolysis [57,58].

The fixed carbon concentrations of the untreated and treated CP were 5.9 and 18.2%, respectively. The results of this study indicate that treated CP has a higher fixed carbon than untreated CP. This finding aligns with previous studies that found an increase in fixed carbon concentration following biomass hydrolysis. The increase can be attributed to the removal of inorganic materials, resulting in a decrease in ash content [48,59].

Figure 2B depicts the ultimate analysis of untreated and treated CP showing carbon, hydrogen, nitrogen, sulfur, and oxygen relative abundances. The values observed for all elements (except oxygen) are consistent with previous literature. Carbon concentration has been reported in the range of 36.96% [60] to 54.9% [48], hydrogen concentration in the range of 3.98 [60] to 10.19 [48], nitrogen concentration in the range of 0.26 [48] to 3.32 [60], sulphur concentration in the range of 0.04 to 0.18 [50], and oxygen concentration in the range of 32.27 [48] to 44.68 [50]. The presence of sulfur in the treated sample

can be attributed to the diffusion of sulphuric acid into the biomass during the acid hydrolysis process [61]. Furthermore, the emergence of a new peak in the DTG spectra at 105 °C (Figure 1B), potentially associated with the degradation of light compounds, further supports the presence of new sulfur groups in the sample.

3.1.3 Functional group analysis

Untreated and treated CP were characterized using FT-IR to determine the alterations in functional groups that occurred following acid hydrolysis. CP, being a biomass source with high amounts of both starch and lignocellulosic material, is a rich source of functional groups, including but not limited to alcohols, ketones, and aromatics [62]. Figure 3 depicts the corresponding spectra whereby the emergence of distinctive absorption peaks can be observed. Some shifts in the peak position were also observed when comparing the untreated and treated CP.

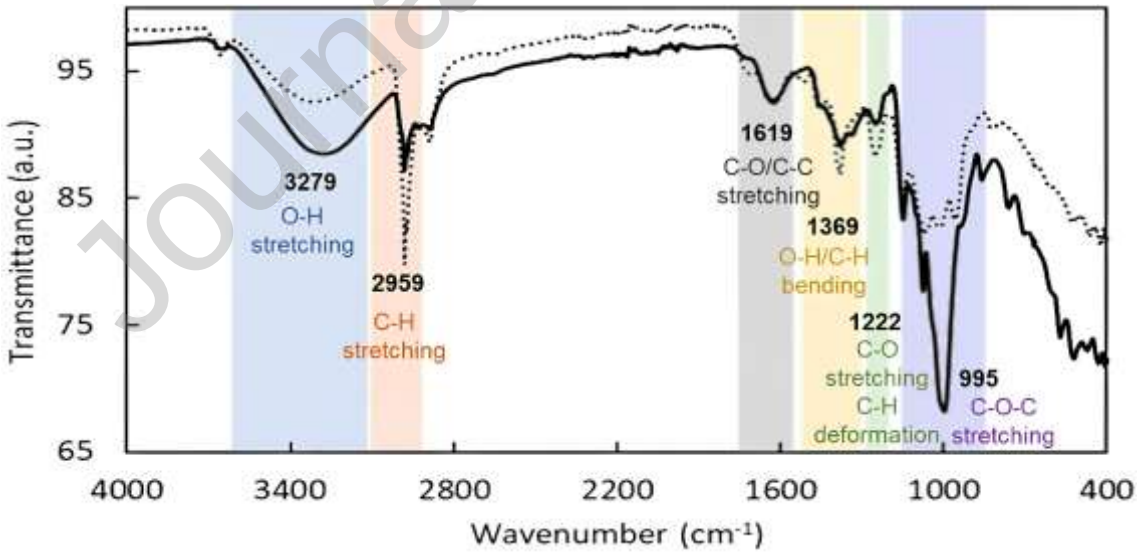

Figure 3. FT-IR spectra of untreated (black line) and treated (dotted line) cassava peel.

The peak observed at 3279 cm^{-1} corresponds to the O-H stretching, which is likely associated with the hydroxylic groups present in both starch and cellulose [54,62]. The reduction in the peak intensity in the treated sample might be linked to the reduced moisture content and is in line with the results presented in Figure 2A. It has been proposed that this peak may be a result of sample dehydration [42]. The presence of a distinct peak at 2959 cm^{-1} suggests the stretching vibration of C-H in CH_2 and CH_3 groups that are present in starch, cellulose, hemicellulose, and lignin [63]. The intensified peak in the treated sample could be due to the solubilisation of starch, cellulose, and hemicellulose in the form of fermentable sugars following acid hydrolysis [63]. The peak detected at 1619 cm^{-1} indicates the existence of C=O and C=C functional groups, which are present in hemicellulose and lignin [47,62]. This peak may also be attributed to the carbonyl groups in the starch chain [63]. The peak detected at 1369 cm^{-1} may represent the O-H bending vibration of starch and cellulose [64]. Additionally, it may also be associated with the C-H bending vibration of the carboxylic groups [47]. The peak observed at 1222 cm^{-1} may correspond to the C-O stretching of hemicellulose and lignin, as well as the deformation of C-H in aromatic rings [47]. The increase of this peak may be due to the presence of pseudo-lignin, which is formed through the re-polymerization of degradation products of polysaccharides. The formation of pseudo-lignin is a characteristic phenomenon associated with dilute acid hydrolysis [65]. The signal detected at 995 cm^{-1}, which exhibits the largest intensity in the untreated cassava peels disappears entirely following acid treatment, and might be associated with the C-O-C stretching of the β-glycosidic linkage in cellulose.

The absence of this peak in the treated sample may be due to the breakdown of cellulose into reducing sugars during the acid hydrolysis process.

Aruwajoye et al. conducted an analysis of the functional groups of cassava peels before and after an acid pre-treatment using 3.68 v/v HCl, for 2.57 h and at 69.62 ºC [54] and confirmed that acid hydrolysis alters the structural composition and properties of CP. The acidic environment leads to the cleavage of the chemical bonds in polysaccharides; resulting in an increased concentration of smaller molecules, such as reducing sugars, and a reduced concentration of polysaccharides and larger molecules such as starch, cellulose, hemicellulose, and lignin [66]. Furthermore, other structures, such as pseudo-lignin, can be formed due to a repolymerization process. The impact of different hydrolysis conditions (e.g., acid concentration, hydrolysis time, hydrolysis temperature, etc.) on CP can result in differences in the biomass degradation, resulting for example in variable presence of reducing sugars hence, affecting the process yields whilst affecting the structural integrity and properties of the resulting hydrolysate.

3.1.4 Surface morphology analysis

Scanning Electron Microscopy (SEM) was employed to characterize the surface of untreated and treated CP (Figure 4).

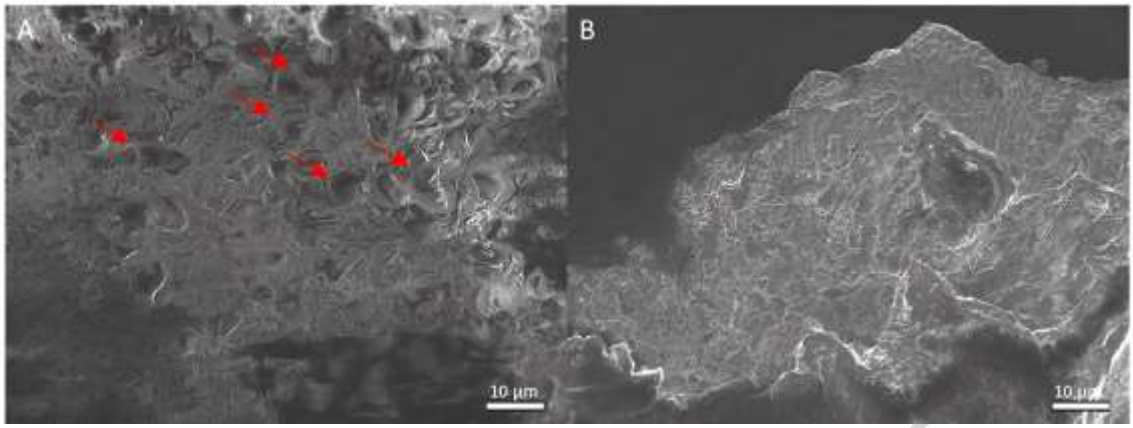

Figure 4. Scanning electron microscopy (SEM) of (A) untreated, and (B) treated cassava peel. Red arrows indicate some of the starch granules.

Starch granules can be observed in the untreated CP, which contributes to the non-uniform surface of the sample. This result is supported by previous authors, who observed globular starch granules covering the surface of cassava peel [67]. However, starch granules are less noticeable, in the treated CP, indicating the effect of the acid pre-treatment in breaking down the polysaccharides. Aruwajoye et al. observed a similar effect upon acid and thermal pre-treatment of CP. Our results confirm the surface structural changes in polysaccharides resulting from acid hydrolysis, as it offers detailed images of the surface morphology of biomass.

The surface morphology analysis together with the TGA, proximate, ultimate, and functional group analysis presented in this study offers a comprehensive evaluation of the structural differences between untreated and acid hydrolysed CP. The results confirm the degradation of intricate polysaccharides into smaller, more readily fermentable sugars after acid pretreatment. Consequently, this pre-treatment method enables the subsequent conversion of these sugars into value-added products, thereby resulting in the valorisation of CP waste.

3.2 Optimization of cassava peel hydrolysis

RSM is a useful tool comprised of mathematical and statistical techniques commonly used to optimize one or several responses of a process [37]. To reduce the number of experimental trials, a CCD was performed to determine the optimum conditions for the hydrolysis of CP. The effect of the three variables on the TRS concentration in the hydrolysate was investigated: H_2SO_4 concentration, hydrolysis time, and hydrolysis temperature. The experimental design matrix and response values are shown in Table 2.

Table 2. Central Composite Design matrix cassava peel hydrolysis along with the response (total reducing sugars, TRS) values.

Run	Factor x_1 [H_2SO_4] (M)	Factor x_2 Time (min)	Factor x_3 Temperature (°C)	Response TRS concentration (g/L)
1	-1	1	-1	17.1
2	-1	1	1	62.0
3	-1	-1	1	82.1
4	-1	-1	-1	14.2
5	1	-1	1	72.1
6	1	-1	-1	37.9
7	1	1	-1	82.1
8	1	1	1	60.0
9	-1.68	0	0	3.5
10	1.68	0	0	85.7
11	0	-1.68	0	77.0
12	0	0	-1.68	12.4
13	0	0	1.68	72.9
14	0	1.68	0	78.3
15	0	0	0	66.4
16	0	0	0	65.0
17	0	0	0	54.6
18	0	0	0	73.4
19	0	0	0	66.3
20	0	0	0	72.1

Results presented in Table 2 were analysed by Design Expert using ANOVA and the fitted equation model was obtained. Table 3 shows the results of the ANOVA, which indicate that the model is significant, with an F-value of 28.55 and a p-value lower than 0.0001. These values imply that an F-value of this magnitude is only 0.01% likely to occur due to noise. Furthermore, the F-value 0.9404 and p-value 0.5101 of the lack of fit imply that this is not significant relative to the pure error. Since the fit of the model is desirable, the insignificance of the lack of fit means that the model has good predictability. The coefficient of variation (CV) is 13.14% and lies below an acceptable limit of 15% [68]. The fitness of the model was assessed by the coefficient of determination R^2 (0.9694). This value indicates that the variables account for more than 96% of the variation and that the model cannot explain less than 4% of the total variance. Adequate precision measures the signal-to-noise ratio and values greater than 4 are desirable. The ratio of 16.2 indicates that the signal for the model is adequate which can be used to navigate the design space. The adjusted R^2 (0.9147) is in reasonable agreement with the predicted R^2 (0.8003), showing a difference lower than 0.2 [37].

Table 3. Analysis of variance (ANOVA) of the central composite design reduced cubic model.

Source	Sum of squares	df	Mean square	F-value	p-value
Model	12442.36	10	12442.36	28.55	<0.0001
x_1	3406.78	1	3406.78	78.18	<0.0001
x_3	3787.83	1	3787.83	86.92	<0.0001
x_1x_2	303.32	1	303.32	6.96	0.0270
x_1x_3	1267.06	1	1267.06	29.08	0.0004
x_2x_3	789.63	1	789.63	18.12	0.0021
x_1^2	890.83	1	890.83	20.44	0.0014

x_3^2	1047.60	1	1047.60	24.04	0.0008
$x_1x_2^2$	759.42	1	759.42	17.43	0.0024
Residual	692.21	9	692.21	-	-
Lack of fit	168.38	4	168.38	0.9404	0.5101
Pure error	223.83	5	223.83	-	-
Cor Total	12834.57	19	12834.57	-	-

C.V = 13.14%; R^2 = 0.9694; Adj R^2 = 0.9147; Pred R^2 = 0.8003; Adeq Precision = 16.2130. x_1: H_2SO_4 concentration; x_2: time; x_3: temperature

Table 3 also shows the statistics of the individual factors and the interactions between them, which were used to build the polynomial model equation. Equation 9 (Eq. 9) shows the enhanced polynomial model for the estimation of TRS concentration:

$$y=69.49+24.85x_1+16.69x_3+6.16x_1x_2-12.59x_1x_3-9.94x_2x_3-8.39x_1^2-8.96x_3^2-15.25x_1x_2^2 \quad \text{(Eq. 9)}$$

The coefficient sign (+/-) defines the direction of the relationship between each of the factors and the response. A positive coefficient means that as the value of the independent variable increases, the dependent variable will also increase. A negative coefficient indicates that as the independent variable rises, the dependent variable falls [69]. Table 3 shows that H_2SO_4 concentration and temperature poses significant linear, quadratic, and interactive effects on the model. The linear (x_2) and quadratic (x_2^2) coefficients for time were removed from the model due to their non-significance. However, the interactions of time with H_2SO_4 concentration and temperature (x_1x_2, x_2x_3, and $x_1x_2^2$) produced p-values below 0.05 indicating their significance to the model.

In conclusion, the ANOVA analysis confirms the significance and good predictability of the fitted equation model. The obtained results, indicate that the variables accounted for a significant proportion of the variation and the model can be reliably used for navigating the design space.

The predicted *vs.* actual values plot (Figure 5A) shows that the predicted values agree with the experimental results. All points lie very close to the line, indicating an excellent fit where x=y. The strong fit of this model confirms that the reduced cubic model can be used to estimate and optimize the TRS concentration in the CPH.

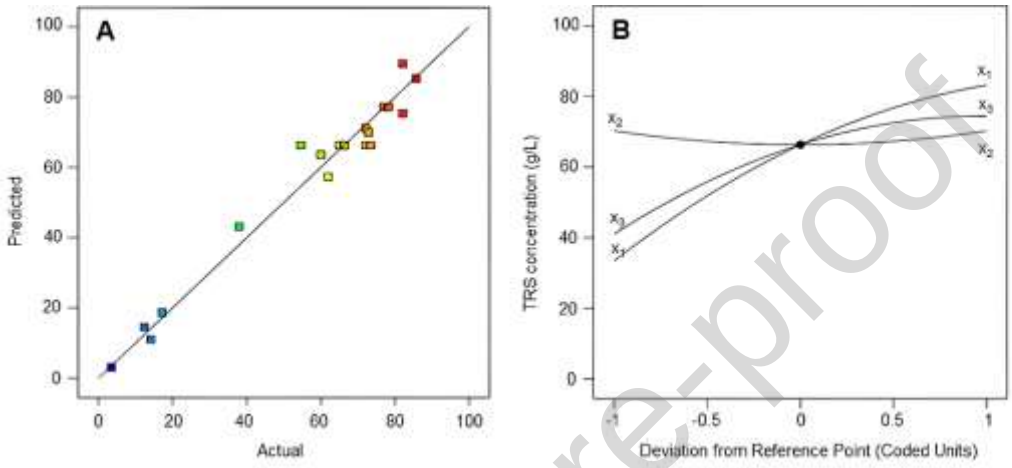

Figure 5. (A) Total reducing sugars (TRS) concentration predicted vs. actual values plot; (B) Perturbation plot over TRS concentration (g/L). (x_1) H_2SO_4 concentration; (x_2) time; (x_3) temperature.

Results shown in Figure 5B examines the single effect of the three factors involved in the design. As can be observed, the increase in H_2SO_4 concentration and temperature leads to an increase in TRS concentration. However, time shows a reduced effect at all ranges, confirming its non-significance in the model as a single factor.

The analysis of the interactions between variables was further investigated based on the contour and 3D response surface plots, as presented in Figure 6.

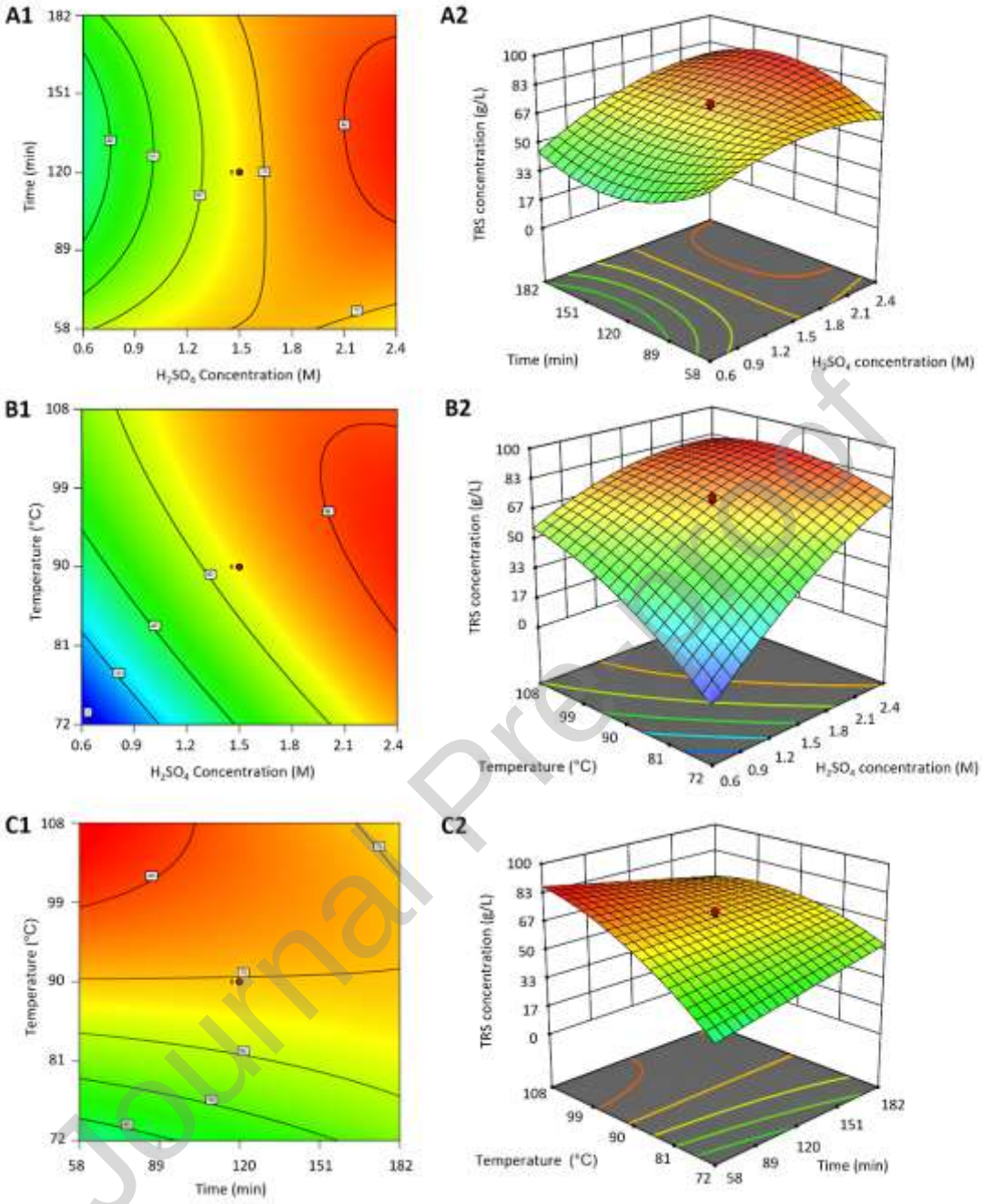

Figure 6. Contour plots (1) and 3D response surface plots (2) representing the effect of (A), H_2SO_4 concentration (M) and time (min); (B), H_2SO_4 concentration (M) and temperature (ºC); and (C), time (min) and temperature (ºC); over total reducing sugars (TRS) concentration (g/L).

Each pair of plots (A, B, and C) shows the response as a function of two parameters while maintaining the third parameter at a fixed central level. As can be seen, TRS concentrations exceeding 80 g/L can be achieved through various combinations of the independent variables. Figure 6A illustrates the interaction between H_2SO_4 concentration and time, where the highest TRS concentration can be obtained by using H_2SO_4 higher than 2 M with reaction times between 90 and 175 min. Figure 6B shows the interaction between H_2SO_4 concentration and temperature, where H_2SO_4 concentrations higher than 2 M and temperatures ranging from 80 ºC to 105 ºC yields TRS concentrations higher than 83 g/L. Finally, Figure 6C shows the interaction between temperature and time, indicating that the maximum TRS concentration can be achieved by using temperatures exceeding 99 ºC within 90 min. Overall, our results indicate that increasing H_2SO_4 concentration and temperature leads to higher TRS concentration. Therefore, it can be concluded that the duration of the hydrolysis reaction, in combination with the other two independent variables, has a significant impact on the TRS concentration. Onyelucheya and co-workers used H_3PO_4 to hydrolyse CP and found that increasing the acid concentration led to a reduction in the required hydrolysis time [34]. However, their study did not provide a systematic approach to optimize the hydrolysis of CP nor explore optimal conditions. In contrast, our study, employing a DoE approach, revealed a more intricate interaction between acid concentration and hydrolysis time. The analysis of the 3D and contour plots presented in Figure 6 revealed that H_2SO_4 concentrations from 2 M, time between 70 and 175 min, and hydrolysis temperatures from 85 °C yield over 80 g/L of TRS.

We carried out an independent experiment to validate our model employing 2.2 M H_2SO_4, 150 min reaction time, and 102 °C, achieving 80.31 g/L of TRS. The predicted TRS concentration was 80.71 g/L, being an acceptable error of 0.5% between the experimental and the predicted value.

Considering the carbohydrate concentration of 88% in CP [30], a maximum conversion of 97% of carbohydrates into reducing sugars was achieved in the CPH in this study. Upon comparison with other studies, hydrolysis with H_2SO_4 has been reported to yield 66 and 94% of TRS conversion from cassava peel at t 110 °C [14] and 135 °C [13], respectively. Nevertheless, these works show disparities in the optimal concentration of acid and did not conduct a systematic study. Our research shows that H_2SO_4 concentrations higher than 2 M and temperatures around 85 °C lead to conversion yields of 97%. Ajala and co-workers reported an optimum H_2SO_4 concentration of 1.5 M to achieve 94% conversion, being in close agreement with our findings [14]. In contrast, Yoonan and Kongkiattikajorn report 0.1 M H_2SO_4 as the optimal concentration for the hydrolysis of cassava peels. However, the authors only achieved 66% conversion [13], significantly lower than our results. Focusing on the reaction time, we found that conducting the hydrolysis between 70 to 175 min leads to conversions up to 97%. The aforementioned studies used hydrolysis times of 120 min and 90 min respectively [13,14]. Nevertheless, the optimization of the process variable time and the interaction of the three different factors was not described. While our process requires slightly higher concentrated H_2SO_4, theirs employ a higher temperature. The interest in using lower temperatures and times is not only due to the lower energy demand but also to the mitigation of glucose degradation. High temperatures and prolonged reaction times can

lead to the degradation of glucose, which may lead to lower conversion yields [34]. Furthermore, our study employs a systematic optimization approach, considering three variables simultaneously, whereas the study performed by Ajala and co-workers employed a fixed time [14].

The present study was optimised to hydrolyse cassava peel using H_2SO_4 as the catalyst, achieving a maximum conversion of 97% from CP to TRS. To the best of the authors knowledge, this is the highest conversion reported to date. Other acids can be used to show similar conversion rates. Various authors report varying concentrations of HCl achieving 94.5 and 93% of conversion [32,54]. It is important to consider that the variations in yields may be attributed to the feedstock variability, as well as differences in the acid used, concentration, reaction time, and temperature. For example, due to its chemical structure, starch is more easily digestible than cellulose and hemicellulose. This is because the α-1,4 and α-1,6 glycosidic bonds of starch are not as strong as the β-1.4-glycosidic bonds of cellulose and hemicellulose, hence they are more resistant to dilute acids. Therefore, the hydrolysis of cellulose and hemicellulose usually requires more severe conditions than starch [70]. Some authors have suggested that the total conversion of cellulose and hemicellulose into reducing sugars is not possible [71], which may explain the presence of 3% undegraded carbohydrates in our study. To the best of our knowledge, our study yields the highest conversion rate of cassava to reducing sugars, via a systematic optimization study.

3.3 Screening of microbial growth and PHA production from CPH

The 15 different CPH obtained from the hydrolysis experiments with different TRS concentrations (Table 2) were utilised to screen the growth of *C. necator* and its ability to produce PHA (Figure 7). Results are presented after 48h of culture, indicating that *C. necator* was able to metabolise all the CPH to different extents and produce PHA at varying levels. Growth varied from OD_{600} 0.7 using the CPH (1.5 M H_2SO_4, 15 min and 90ºC), to OD_{600} as high as 15.8 using the CPH (0.6 M H_2SO_4, 58 min and 107 ºC). The latter value is comparable to experiments using 10 g/L of commercial glucose as the carbon source whereby OD_{600} 16 was achieved after 48h of culture. With OD_{600} values of 14.4; 15.3 and 15.8 (Figure 7A), three out of the 15 experiments showed growth comparable to the cultures using synthetic glucose. To understand what might be affecting the microbial growth in the experiments presenting lower growth, different factors such as substrate inhibition and volume of alkali were analysed [94]. Substrate inhibition was disregarded in our study since Figure 7B shows that the culture that produced the greatest growth corresponds to the CPH that contained the highest amount of TRS, 75.2 g/L. The initial sugar concentration in the culture had no beneficial impact on the growth either. The culture presenting OD_{600} 14.4 had a starting TRS concentration of 27.6 g/L. Nevertheless, the CPH (1.5 M H_2SO_4, 15 min, and 90 ºC) resulted in OD_{600} lower than 1, having an initial sugar concentration of 66.4 g/L.

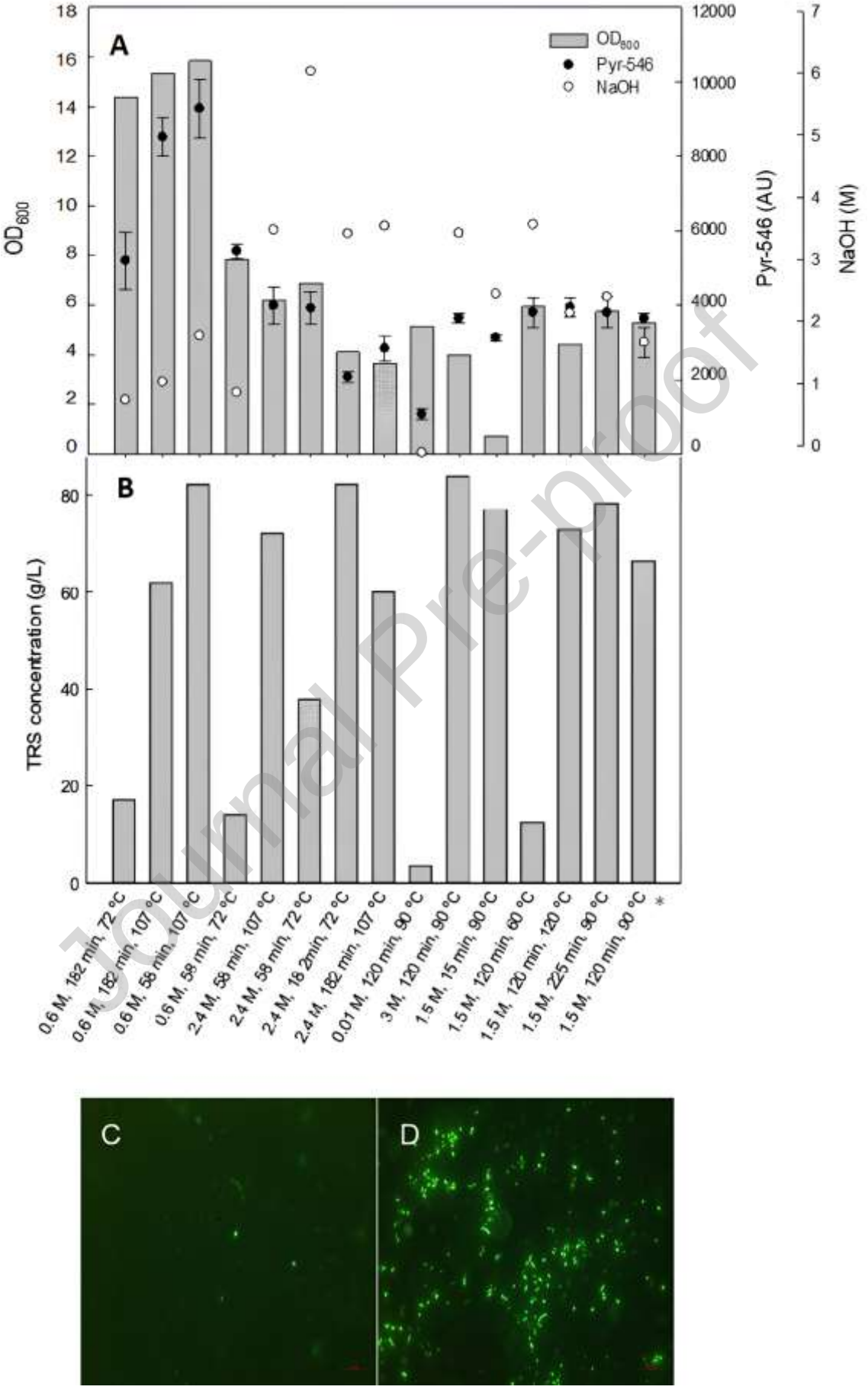

Figure 7. Screening of *C. necator* growth and PHA production using different cassava peel hydrolysates (CPH). Grey column, OD_{600}; (●) Relative fluoresce values of pyr-546-stained cells measured by Flow cytometry and corresponding to PHA content (n=3) and (○) NaOH (M) used for CPH neutralization (A); Total reducing sugars (TRS) concentration (B) obtained from each hydrolysis condition. (*) Average and standard deviation values are given for the central point (1.5M, 120min, and 90 °C) (B); Fluorescence microscopy images of Pyro-546-stained cells indicating polyhydroxyalkanoates (PHA) production in CPH from a representative experiment obtained under hydrolysis conditions of 0.01 M, 120 min and 90 ºC (C); and 0.6 M, 58 min and 107 ºC (D).

Figure 7A shows the concentration of alkali used to neutralise the culture media and its impact on microbial growth. All the CPH obtained using 0.6 M presented the highest growth results. All these experiments required NaOH concentrations lower than 2 M to be neutralised. Cultures that needed less alkali grew more on average. CPH (0.01 M H_2SO_4, 120 min, and 90 ºC) did not require a neutralisation step. However, the growth only reached OD_{600} 5.15. This might be a result of the low availability of TRS in the media, being 3.5 g/L. The more alkaline solution is added to an acidic solution, the higher is likelihood that salts will be formed in the media, and high salt concentrations may prevent bacterial growth [72]. To the best of the author's knowledge, this study presents the pioneering investigation of *C. necator* growth through a comprehensive screening utilising various CPH. The findings of this research provide a benchmark for the utilisation of CPH and serve as a valuable reference for future studies in this area.

FCM was used to rapidly assess relative PHA, specifically PHBV, content within individual bacteria by staining with the lipophilic fluorophore pyr-546 [73]. This dye has the ability to enter bacteria and stain PHA green. As shown in the correlation between PHA concentration (%) quantified using GC-MS and fluorescence values from FCM, higher fluorescence values mean higher PHA content (supplementary materials).

Figure 7C and 7D represents a fluorescence microscope image showing representative samples with low and high fluorescence values of pyro-546-stained cells grown on CPH (0.01 M, 120 min, and 90 ºC) and CPH (0.6 M, 58 min and 107 ºC), corresponding to PHA accumulation of 10 and 31 % PHA (g_{PHA}/g_{DCW}), equivalent to 0.15 and 1.5 g/L of PHA, respectively. Therefore, we have employed FCM analysis as a rapid and high throughput method to screen and confirm the potential of *C. necator* to produce PHA from CPH. Vega-Castro and co-workers reported the production of 0.064 g/L of PHA using acid-hydrolysed cassava peels [74]. Our work whereby 31% PHA corresponds to 1.38 g/L of PHA, clearly shows improved yields than the previously published. Furthermore, to the best of our knowledge, the application of FCM for assessing PHA production from CP has not been previously reported. The use of FCM in this study confirmed the ability of *C. necator* to produce PHA from CPH.

4. Conclusions

We developed an integrated strategy for converting waste into PHA using chemical and biological conversion technologies. Comparison of acid-untreated and treated CP revealed thermal, physicochemical, and morphological changes. Our optimization study achieved the highest conversion value using a systematic study, to the best of the author's knowledge. Screening using CPH

demonstrated the ability of *C. necator* to produce PHA and showed the high potential of biomass waste to be valorised into high-value bioproducts. This work contributes to the sustainable and integrated development of biorefinery systems using biomass waste contributing to meeting Net Zero targets.

Author contributions

The authors confirm contribution to the paper as follows: Carmen Hierro-Iglesias: Investigation, methodology, funding acquisition, writing-original draft, and review and editing. Cornelius O. Fatokun: Investigation, methodology, and review and editing. Annie Chimphango: supervision, funding acquisition, and writing-review and editing. Richard Bayitse: methodology writing-review and editing. Paula Helena Blanco-Sanchez: methodology and formal analysis. Patricia Thornley: supervision, funding acquisition, and writing-review and editing. Alfred Fernandez-Castane: conceptualisation, funding acquisition supervision, and writing-review and editing. All authors approved the final version of the manuscript.

Declaration of interests

☒ The authors declare that they have no known competing financial interests or personal relationships that could have appeared to influence the work reported in this paper.

☐ The authors declare the following financial interests/personal relationships which may be considered as potential competing interests:

Acknowledgments

Carmen Hierro Iglesias acknowledges the College of Engineering and Physical Sciences at Aston University for her PhD studentship.

Declaration of Competing Interest

The authors declare that they have no known competing financial interests or personal relationships that could have appeared to influence the work reported in this paper.

References

[1] E. de Jong, A. Higson, P. Walsh, M. Wellisch, Task 42 Biobased Chemicals - Value Added Products from Biorefineries, 2011.

[2] J. Poore, T. Nemecek, Reducing food's environmental impacts through producers and consumers, Science (1979). 360 (2018) 987–992. https://doi.org/10.1126/science.aaq0216.

[3] S. Sielhorst, J.W. Molenaar, D. Offermans, Biofuels in Africa: an assessment of risks and benefits for African wetlands, 2008.

[4] Preethi, G. M., G. Kumar, O.P. Karthikeyan, S. Varjani, R.B. J., Lignocellulosic biomass as an optimistic feedstock for the production of biofuels as valuable energy source: Techno-economic analysis, Environmental Impact Analysis, Breakthrough and Perspectives, Environ Technol Innov. 24 (2021) 102080. https://doi.org/10.1016/j.eti.2021.102080.

[5] S. Sivamani, A.P. Chandrasekaran, M. Balajii, M. Shanmugaprakash, A. Hosseini-Bandegharaei, R. Baskar, Evaluation of the potential of cassava-based residues for biofuels production, Rev Environ Sci Biotechnol. 17 (2018) 553–570. https://doi.org/10.1007/s11157-018-9475-0.

[6] C. Hierro-Iglesias, A. Chimphango, P. Thornley, A. Fernández-Castané, Opportunities for the development of cassava waste biorefineries for the production of polyhydroxyalkanoates in Sub-Saharan Africa, Biomass Bioenergy. 166 (2022) 106600. https://doi.org/10.1016/j.biombioe.2022.106600.

[7] N. Poomipuk, A. Reungsang, P. Plangklang, Poly-β-hydroxyalkanoates production from cassava starch hydrolysate by Cupriavidus sp. KKU38, Int J Biol Macromol. 65 (2014) 51–64. https://doi.org/10.1016/j.ijbiomac.2014.01.002.

[8] A. Anukam, J. Berghel, Biomass Pretreatment and Characterization: A Review, in: Biotechnological Applications of Biomass, IntechOpen, 2021. https://doi.org/10.5772/intechopen.93607.

[9] J. Cai, Y. He, X. Yu, S.W. Banks, Y. Yang, X. Zhang, Y. Yu, R. Liu, A. V. Bridgwater, Review of physicochemical properties and analytical characterization of lignocellulosic biomass, Renewable and Sustainable Energy Reviews. 76 (2017) 309–322. https://doi.org/10.1016/j.rser.2017.03.072.

[10] R. García, C. Pizarro, A.G. Lavín, J.L. Bueno, Characterization of Spanish biomass wastes for energy use, Bioresour Technol. 103 (2012) 249–258. https://doi.org/10.1016/j.biortech.2011.10.004.

[11] T.R. Sarker, R. Azargohar, A.K. Dalai, M. Venkatesh, Physicochemical and Fuel Characteristics of Torrefied Agricultural Residues for Sustainable Fuel Production,

Energy & Fuels. 34 (2020) 14169–14181. https://doi.org/10.1021/acs.energyfuels.0c02121.

[12] A. Anukam, S. Mamphweli, P. Reddy, E. Meyer, O. Okoh, Pre-processing of sugarcane bagasse for gasification in a downdraft biomass gasifier system: A comprehensive review, Renewable and Sustainable Energy Reviews. 66 (2016) 775–801. https://doi.org/10.1016/j.rser.2016.08.046.

[13] K. Yoonan, J. Kongkiattikajorn, A Study of Optimal Conditions for Reducing Sugars Production, Kasetsart Journal: Natural Science. 35 (2004) 29–35.

[14] E.O. Ajala, M.A. Ajala, I.A. Tijani, A.A. Adebisi, I. Suru, Kinetics modelling of acid hydrolysis of cassava (Manihot esculanta Cranz) peel and its hydrolysate chemical characterisation, J King Saud Univ Sci. 32 (2020) 2284–2292. https://doi.org/10.1016/j.jksus.2020.03.003.

[15] A. Steinbüchel, B. Füchtenbusch, Bacterial and other biological systems for polyester production, Trends Biotechnol. 16 (1998) 419–427. https://doi.org/10.1016/S0167-7799(98)01194-9.

[16] D. Jendrossek, R. Handrick, Microbial degradation of polyhydroxyalkanoates, Annu Rev Microbiol. 56 (2002) 403–432. https://doi.org/10.1146/annurev.micro.56.012302.160838.

[17] D. Jendrossek, D. Pfeiffer, New insights in the formation of polyhydroxyalkanoate granules (carbonosomes) and novel functions of poly(3-hydroxybutyrate), Environ Microbiol. 16 (2014) 2357–2373. https://doi.org/10.1111/1462-2920.12356.

[18] A. Fernández-Castané, H. Li, O.R.T. Thomas, T.W. Overton, Flow cytometry as a rapid analytical tool to determine physiological responses to changing O2 and iron concentration by Magnetospirillum gryphiswaldense strain MSR-1, Sci Rep. 7 (2017) 1–11. https://doi.org/10.1038/s41598-017-13414-z.

[19] C. Hierro-Iglesias, M. Masó-Martínez, J. Dulai, K.J. Chong, P.H. Blanco-Sanchez, A. Fernández-Castané, Magnetotactic Bacteria-Based Biorefinery: Potential for Generating Multiple Products from a Single Fermentation, ACS Sustain Chem Eng. 9 (2021) 10537–10546. https://doi.org/10.1021/acssuschemeng.1c02435.

[20] S. Obruca, P. Sedlacek, E. Slaninova, I. Fritz, C. Daffert, K. Meixner, Z. Sedrlova, M. Koller, Novel unexpected functions of PHA granules, Appl Microbiol Biotechnol. 104 (2020) 4795–4810. https://doi.org/10.1007/s00253-020-10568-1.

[21] J.P. Greene, Degradation and Biodegradation Standards for Biodegradable Food Packaging Materials, in: Reference Module in Food Science, Elsevier, 2019. https://doi.org/10.1016/B978-0-08-100596-5.22437-2.

[22] E. Bugnicourt, P. Cinelli, A. Lazzeri, V. Alvarez, Polyhydroxyalkanoate (PHA): review of synthesis, characteristics, processing and potential applications in packaging, Express Polym Lett. 8 (2014) 791–808. https://doi.org/10.3144/expresspolymlett.2014.82.

[23] W. Chen, Y.W. Tong, PHBV microspheres as neural tissue engineering scaffold support neuronal cell growth and axon–dendrite polarization, Acta Biomater. 8 (2012) 540–548. https://doi.org/10.1016/j.actbio.2011.09.026.

[24] C.S. Wu, Controlled release evaluation of bacterial fertilizer using polymer composites as matrix, Journal of Controlled Release. 132 (2008) 42–48. https://doi.org/10.1016/j.jconrel.2008.08.015.

[25] M. Kumar, R. Rathour, R. Singh, Y. Sun, A. Pandey, E. Gnansounou, K.-Y. Andrew Lin, D.C.W. Tsang, I.S. Thakur, Bacterial polyhydroxyalkanoates: opportunities, challenges, and prospects, J Clean Prod. 263 (2020) 121500. https://doi.org/10.1016/j.jclepro.2020.121500.

[26] B.H.A. Rehm, Polyester synthases: natural catalysts for plastics, Biochemical Journal. 376 (2003) 15–33. https://doi.org/10.1042/BJ20031254.

[27] K. Wang, A.M. Hobby, Y. Chen, A. Chio, B.M. Jenkins, R. Zhang, Techno-Economic Analysis on an Industrial-Scale Production System of Polyhydroxyalkanoates (PHA) from Cheese By-Products by Halophiles, Processes. 10 (2021) 17. https://doi.org/10.3390/pr10010017.

[28] K.Y. Sen, M.H. Hussin, S. Baidurah, Biosynthesis of poly(3-hydroxybutyrate) (PHB) by Cupriavidus necator from various pretreated molasses as carbon source, Biocatal Agric Biotechnol. 17 (2019) 51–59. https://doi.org/10.1016/j.bcab.2018.11.006.

[29] A. Getachew, F. Woldesenbet, Production of biodegradable plastic by polyhydroxybutyrate (PHB) accumulating bacteria using low cost agricultural waste material, BMC Res Notes. 9 (2016) 509. https://doi.org/10.1186/s13104-016-2321-y.

[30] R. Bayitse, X. Hou, A.-B. Bjerre, F.K. Saalia, Optimisation of enzymatic hydrolysis of cassava peel to produce fermentable sugars, AMB Express. 5 (2015) 60. https://doi.org/10.1186/s13568-015-0146-z.

[31] M. Asadieraghi, W.M.A. Wan Daud, Characterization of lignocellulosic biomass thermal degradation and physiochemical structure: Effects of demineralization by diverse acid solutions, Energy Convers Manag. 82 (2014) 71–82. https://doi.org/10.1016/j.enconman.2014.03.007.

[32] A.L. Woiciechowski, S. Nitsche, A. Pandey, C.R. Soccol, Acid and enzymatic hydrolysis to recover reducing sugars from cassava bagasse: an economic study, Brazilian Archives of Biology and Technology. 45 (2002) 393–400. https://doi.org/10.1590/S1516-89132002000300018.

[33] A.A. Olanbiwoninu, S.A. Odunfa, Enhancing the Production of Reducing Sugars from Cassava Peels by Pretreatment Methods, 2 (2012).

[34] O.E. Onyelucheya, J.T. Nwabanne, C.M. Onyelucheya, O.E. Adeyemo, Acid Hydrolysis Of Cassava Peel, 5 (2016) 184–187.

[35] N.S. Neta, A.M. Peres, J.A. Teixeira, L.R. Rodrigues, Maximization of fructose esters synthesis by response surface methodology, N Biotechnol. 28 (2011) 349–355. https://doi.org/10.1016/j.nbt.2011.02.007.

[36] S. Dong, M.J. Bortner, M. Roman, Analysis of the sulfuric acid hydrolysis of wood pulp for cellulose nanocrystal production: A central composite design study, Ind Crops Prod. 93 (2016) 76–87. https://doi.org/10.1016/j.indcrop.2016.01.048.

[37] D.C. Montgomery, MONT, in: Catalysis from A to Z, Wiley, 2020. https://doi.org/10.1002/9783527809080.cataz11063.

[38] G.L. Miller, Use of Dinitrosalicylic Acid Reagent for Determination of Reducing Sugar, Anal Chem. 31 (1959) 426–428. https://doi.org/10.1021/ac60147a030.

[39] V. Riis, W. Mai, Gas chromatographic determination of poly-β-hydroxybutyric acid in microbial biomass after hydrochloric acid propanolysis, J Chromatogr A. 445 (1988) 285–289. https://doi.org/10.1016/S0021-9673(01)84535-0.

[40] L. Hu, X.-Y. Wei, X.-H. Guo, H.-P. Lv, G.-H. Wang, Investigation on the kinetic behavior, thermodynamic and volatile products analysis of chili straw waste pyrolysis, J Environ Chem Eng. 9 (2021) 105859. https://doi.org/10.1016/j.jece.2021.105859.

[41] A. Al-Rumaihi, P. Parthasarathy, A. Fernandez, T. Al-Ansari, H.R. Mackey, R. Rodriguez, G. Mazza, G. McKay, Thermal degradation characteristics and kinetic study of camel manure pyrolysis, J Environ Chem Eng. 9 (2021). https://doi.org/10.1016/j.jece.2021.106071.

[42] K. Aup-Ngoen, M. Noipitak, Effect of carbon-rich biochar on mechanical properties of PLA-biochar composites, Sustain Chem Pharm. 15 (2020) 100204. https://doi.org/10.1016/j.scp.2019.100204.

[43] N. Paksung, J. Pfersich, P.J. Arauzo, D. Jung, A. Kruse, Structural Effects of Cellulose on Hydrolysis and Carbonization Behavior during Hydrothermal Treatment, ACS Omega. 5 (2020) 12210–12223. https://doi.org/10.1021/acsomega.0c00737.

[44] V. Pasangulapati, K.D. Ramachandriya, A. Kumar, M.R. Wilkins, C.L. Jones, R.L. Huhnke, Effects of cellulose, hemicellulose and lignin on thermochemical conversion characteristics of the selected biomass, Bioresour Technol. 114 (2012) 663–669. https://doi.org/10.1016/j.biortech.2012.03.036.

[45] T.C. Egbosiuba, Biochar and bio-oil fuel properties from nickel nanoparticles assisted pyrolysis of cassava peel, Heliyon. 8 (2022) e10114. https://doi.org/10.1016/j.heliyon.2022.e10114.

[46] S. Sukarni, M.R. Ramadhan, Pyrolytic Characteristics and Kinetic Parameters Evaluation of Cassava Stalks Using Thermogravimetric Analyzer, Key Eng Mater. 851 (2020) 137–141. https://doi.org/10.4028/www.scientific.net/KEM.851.137.

[47] S. Idris, R. Shamsudin, M.Z.M. Nor, M.N. Mokhtar, S.S. Abdul Gani, Physicochemical composition of different parts of cassava (Manihot esculenta Crantz) plant, Food Res. 4 (2020) 78–84. https://doi.org/10.26656/fr.2017.4(S1).S33.

[48] R. Kayiwa, H. Kasedde, M. Lubwama, J.B. Kirabira, Characterization and pre-leaching effect on the peels of predominant cassava varieties in Uganda for production of activated carbon, Current Research in Green and Sustainable Chemistry. 4 (2021) 100083. https://doi.org/10.1016/j.crgsc.2021.100083.

[49] H.I. Owamah, Biosorptive removal of Pb(II) and Cu(II) from wastewater using activated carbon from cassava peels, J Mater Cycles Waste Manag. 16 (2014) 347–358. https://doi.org/10.1007/s10163-013-0192-z.

[50] J. Fonseca, A. Albis, A.R. Montenegro, Evaluation of zinc adsorption using cassava peels (Manihot esculenta) modified with citric acid, Contemporary Engineering Sciences. 11 (2018) 3575–3585. https://doi.org/10.12988/ces.2018.87364.

[51] O.L. Ki, A. Kurniawan, C.X. Lin, Y.H. Ju, S. Ismadji, Bio-oil from cassava peel: a potential renewable energy source, Bioresour Technol. 145 (2013) 157–161. https://doi.org/10.1016/j.biortech.2013.01.122.

[52] M.F. Aller, Biochar properties: Transport, fate, and impact, Crit Rev Environ Sci Technol. 46 (2016) 1183–1296. https://doi.org/10.1080/10643389.2016.1212368.

[53] N.S. Pooja, G. Padmaja, Enhancing the Enzymatic Saccharification of Agricultural and Processing Residues of Cassava through Pretreatment Techniques, Waste Biomass Valorization. 6 (2015) 303–315. https://doi.org/10.1007/s12649-015-9345-8.

[54] G.S. Aruwajoye, F.D. Faloye, E.G. Kana, Soaking assisted thermal pretreatment of cassava peels wastes for fermentable sugar production: Process modelling and optimization, Energy Convers Manag. 150 (2017) 558–566. https://doi.org/10.1016/j.enconman.2017.08.046.

[55] N.S. Pooja, M.S. Sajeev, M.L. Jeeva, G. Padmaja, Bioethanol production from microwave-assisted acid or alkali-pretreated agricultural residues of cassava using separate hydrolysis and fermentation (SHF), 3 Biotech. 8 (2018) 69. https://doi.org/10.1007/s13205-018-1095-4.

[56] M.U. Ude, I. Oluka, P.C. Eze, Optimization and kinetics of glucose production via enzymatic hydrolysis of mixed peels, Journal of Bioresources and Bioproducts. 5 (2020) 283–290. https://doi.org/10.1016/j.jobab.2020.10.007.

[57] P. Alain, K. Nanssou, Y. Jiokap, Pretreatment of cassava stems and peelings by thermohydrolysis to enhance hydrolysis yield of cellulose in bioethanol production process, Renew Energy. 97 (2016) 252–265. https://doi.org/10.1016/j.renene.2016.05.050.

[58] C.O. Ofuya, S.N. Obilor, The suitability of fermented cassava peel as a poultry feedstuff, Bioresour Technol. 44 (1993) 101–104. https://doi.org/10.1016/0960-8524(93)90181-A.

[59] E. Menya, P.W. Olupot, H. Storz, M. Lubwama, Y. Kiros, Characterization and alkaline pretreatment of rice husk varieties in Uganda for potential utilization as precursors in the production of activated carbon and other value-added products, Waste Management. 81 (2018) 104–116. https://doi.org/10.1016/j.wasman.2018.09.050.

[60] C. Tejada-Tovar, A.D. Gonzalez-Delgado, A. Villabona-Ortiz, Characterization of Residual Biomasses and Its Application for the Removal of Lead Ions from Aqueous Solution, Applied Sciences. 9 (2019) 4486. https://doi.org/10.3390/app9214486.

[61] S. Kim, Diffusion of sulfuric acid within lignocellulosic biomass particles and its impact on dilute-acid pretreatment, Bioresour Technol. 83 (2002) 165–171. https://doi.org/10.1016/S0960-8524(01)00197-3.

[62] S. Widiarto, E. Pramono, Suharso, A. Rochliadi, I.M. Arcana, Cellulose Nanofibers Preparation from Cassava Peels via Mechanical Disruption, Fibers. 7 (2019) 44. https://doi.org/10.3390/fib7050044.

[63] G.S. Aruwajoye, F.D. Faloye, E.G. Kana, Process Optimisation of Enzymatic Saccharification of Soaking Assisted and Thermal Pretreated Cassava Peels Waste for Bioethanol Production, Waste Biomass Valorization. 11 (2020) 2409–2420. https://doi.org/10.1007/s12649-018-00562-0.

[64] M.N. Ikhwan Musa, T. Marimuthu, H.N. Mohd Rashid, K.P. Sambasevam, Development of pH indicator film composed of corn starch-glycerol and anthocyanin from hibiscus sabdariffa, Malaysian Journal of Chemistry. 22 (2020) 19–24.

[65] F. Hu, A. Ragauskas, Suppression of pseudo-lignin formation under dilute acid pretreatment conditions, RSC Adv. 4 (2014) 4317–4323. https://doi.org/10.1039/C3RA42841A.

[66] M. Becker, K. Ahn, M. Bacher, C. Xu, A. Sundberg, S. Willför, T. Rosenau, A. Potthast, Comparative hydrolysis analysis of cellulose samples and aspects of its application in conservation science, Cellulose. 28 (2021) 8719–8734. https://doi.org/10.1007/s10570-021-04048-6.

[67] S. Mohd-Asharuddin, N. Othman, N.S. Mohd Zin, H.A. Tajarudin, A Chemical and Morphological Study of Cassava Peel: A Potential Waste as Coagulant Aid, MATEC Web of Conferences. 103 (2017) 06012. https://doi.org/10.1051/matecconf/201710306012.

[68] J.L. Crespo-mariño, E.M. Eds, High performance computing, Aircraft Engineering and Aerospace Technology. 77 (2005) 393–400. https://doi.org/10.1108/aeat.2005.12777dab.008.

[69] N. Boudechiche, H. Yazid, M. Trari, Z. Sadaoui, Valorization of Crataegus azarolus stones for the removal of textile anionic dye by central composite rotatable design using cubic model: optimization, isotherm, and kinetic studies, Environmental Science and Pollution Research. 24 (2017) 19609–19623. https://doi.org/10.1007/s11356-017-9606-0.

[70] J.F. Kennedy, L. Quinton, Essentials of Carbohydrate Chemistry and Biochemistry, Carbohydr Polym. 47 (2002) 87. https://doi.org/10.1016/S0144-8617(01)00274-0.

[71] S. Gámez, J.J. González-Cabriales, J.A. Ramírez, G. Garrote, M. Vázquez, Study of the hydrolysis of sugar cane bagasse using phosphoric acid, J Food Eng. 74 (2006) 78–88. https://doi.org/10.1016/j.jfoodeng.2005.02.005.

[72] D. Kucera, P. Benesova, P. Ladicky, M. Pekar, P. Sedlacek, S. Obruca, Production of polyhydroxyalkanoates using hydrolyzates of spruce sawdust: Comparison of hydrolyzates detoxification by application of overliming, active carbon, and lignite, Bioengineering. 4 (2017). https://doi.org/10.3390/bioengineering4020053.

[73] E. Martinaud, C. Hierro-Iglesias, J. Hammerton, B. Hadad, R. Evans, J. Sacharczuk, D. Lester, M.J. Derry, P.D. Topham, A. Fernandez-Castane, Valorising cassava peel waste into plasticized polyhydroxyalkanoates blended with polycaprolactone with controllable thermal and mechanical properties, J Polym Environ. (2023) IN PRESS.

[74] O. Vega-Castro, E. León, M. Arias, M.T. Cesario, F. Ferreira, M.M.R. da Fonseca, A. Segura, P. Valencia, R. Simpson, H. Nuñez, J. Contreras-Calderon, Characterization and Production of a Polyhydroxyalkanoate from Cassava Peel Waste: Manufacture of Biopolymer Microfibers by Electrospinning, J Polym Environ. 29 (2021) 187–200. https://doi.org/10.1007/s10924-020-01861-1.

Highlights

- Cassava peel (CP) is a renewable resource with great valorisation potential
- Physico-chemical characterisation of CP is key to unlock its valorisation potential
- CP was converted into polyhydroxyalkanoates (PHA) via chemical and microbial routes.
- Optimisation of CP acid hydrolysis resulted in 97% conversion into reducing sugars
- The integration of chemical and biological processes resulted in 31% of PHA
- Flow cytometry allowed rapid, simple and high-throughput assessment of PHA content.